AD-A071 888   HUGHES AIRCRAFT CO   TORRANCE CALIF ELECTRON DYNAMICS DIV   F/G 9/2
                DEVELOPMENT OF A LARGE SIGNAL COMPUTER THEORY FOR TWT.(U)
                JUN 79   T W BERG   F30602-77-C-0221
UNCLASSIFIED   EDO-W-07587   RADC -TR-79-87   NL

| OF |
AD
A071888

END
DATE
FILMED
8 -79
DDC

1.0

4.5
5.0
5.6
6.3

2.8

2.5

1.1

3.2
3.6
4.0

2.2

2.0

1.8

1.25

1.4

1.6

MICROCOPY RESOLUTION TEST CHART

NATIONAL BUREAU OF STANDARDS-1963-A
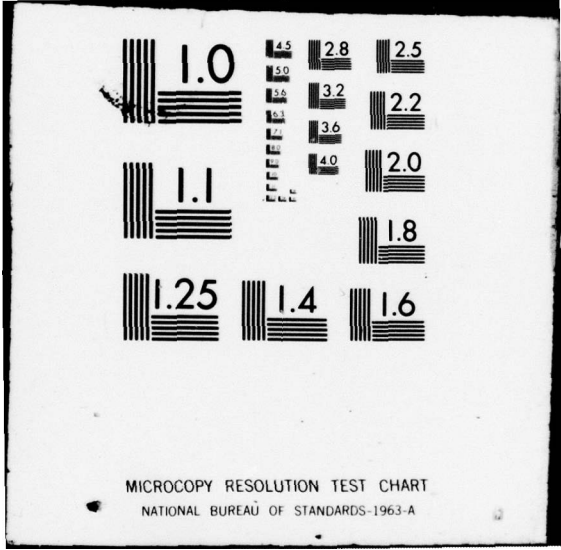
LEVEL

RADC-TR-79-87
Final Technical Report
June 1979

DEVELOPMENT OF A LARGE SIGNAL COMPUTER THEORY FOR TWT

Hughes Aircraft Company

Dr. Tore Wessel Berg

ROME AIR DEVELOPMENT CENTER
Air Force Systems Command
Griffiss Air Force Base, New York 13441

79 07 27 007

This report has been reviewed by the RADC Information Office (OI) and is releasable to the National Information Service (NTIS). At NTIS it will be releasable to the general public, including foreign nations.
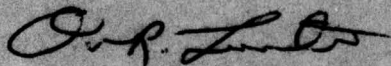
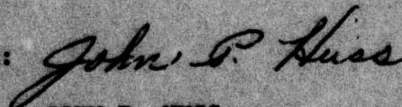RADC-TR-79-87 has been reviewed and is approved for publication.

APPROVED: *[signature]*
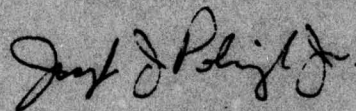
JOSEPH POLNIASZEK
Project Engineer

APPROVED: *[signature]*

OWEN R. LAWTER, Colonel, USAF
Chief, Surveillance Division

FOR THE COMMANDER: *[signature]*

JOHN P. HUSS
Acting Chief, Plans Office

If your address has changed or if you wish to be removed from the RADC mailing list, or if the addressee is no longer employed by your organization, please notify RADC (OCTP), Griffiss AFB NY 13441. This will assist us in maintaining a current mailing list.

Do not return this copy. Retain or destroy.

SECURITY CLASSIFICATION OF THIS PAGE *(When Data Entered)*

REPORT DOCUMENTATION PAGE		READ INSTRUCTIONS BEFORE COMPLETING FORM
1. REPORT NUMBER RADC-TR-79-87	**2. GOVT ACCESSION NO.**	**3. RECIPIENT'S CATALOG NUMBER**
4. TITLE *(and Subtitle)* DEVELOPMENT OF A LARGE SIGNAL COMPUTER THEORY FOR TWT		**5. TYPE OF REPORT & PERIOD COVERED** Final Technical Report. Oct 77 - Nov 78
		6. PERFORMING ORG. REPORT NUMBER W-07587
7. AUTHOR(s) Dr. Tore Wessel-Berg		**8. CONTRACT OR GRANT NUMBER(s)** F30602-77-C-0221
9. PERFORMING ORGANIZATION NAME AND ADDRESS Hughes Aircraft Company, Electron Dynamics Division 3100 West Lomita Boulevard Torrance CA 90509		**10. PROGRAM ELEMENT, PROJECT, TASK AREA & WORK UNIT NUMBERS** 62702F 45061243
11. CONTROLLING OFFICE NAME AND ADDRESS Rome Air Development Center (OCTP) Griffiss AFB NY 13441		**12. REPORT DATE** June 1979
		13. NUMBER OF PAGES 51
14. MONITORING AGENCY NAME & ADDRESS *(if different from Controlling Office)* Same		**15. SECURITY CLASS.** *(of this report)* UNCLASSIFIED
		15a. DECLASSIFICATION/DOWNGRADING SCHEDULE N/A

16. DISTRIBUTION STATEMENT *(of this Report)*

Approved for public release; distribution unlimited.

EDD-W-07587

17. DISTRIBUTION STATEMENT *(of the abstract entered in Block 20, if different from Report)*

Same

18. SUPPLEMENTARY NOTES

RADC Project Engineer: Joseph Polniaszek (OCTP)

19. KEY WORDS *(Continue on reverse side if necessary and identify by block number)*

LARGE SIGNAL THEORY FOR TRAVELING WAVE TUBES BASED ON POLARIZATION VARIABLE FORMULATION

20. ABSTRACT *(Continue on reverse side if necessary and identify by block number)*

The report describes the basic formulations used to express the large signal equations by means of polarization variables, and how these are implemented into a one-dimensional large signal theory of the TWT. The small signal approximation follows as a natural special case which is described by a separate set of equations. The solution of these by means of a separate computer routine gives the small signal response for the TWT and simultaneously furnishes a set of input parameters that are used in the subsequent large signal routine.

(Cont'd)

DD FORM 1 JAN 73 **1473**

402638

20.

The theory is applicable to multisection TWT's, including attenuator sections with heavy loss, provided each section is uniform, in the sense that some of the circuit parameters are varying along each section.

The theory is formulated in such a way as to include general harmonic injection schemes, with injection frequencies up to the third harmonic. This makes possible investigation of efficiency improvements by utilizing the additional degrees of freedom provided by a more general harmonic injection scheme.

The theory is formulated in terms of a set of basic circuit and beam parameters rather than the special TWT parameters used in conventional theory, i.e., the Pierce parameters. The Pierce parameters are not particularly well suited for use in the present model, which differs from the conventional model in several respects. Transformation of the basic parameters used in the present model to the Pierce parameters and vice versa, for interpretation and comparison of results can be done easily subsequent to the computational procedure.

PREFACE

This final technical report was authored by Dr. T. Wessel Berg and prepared by Electron Dynamics Division, Hughes Aircraft Company, Torrance, California on Contract F30602-77-C-0221, for Rome Air Development Center, Griffiss Air Force Base, New York. It summarizes the results of a large signal theory for traveling wave tubes, based on polorization variables, that forms the basis for a new large signal computer program for TWT. This effort has been initiated in October 1977 and was completed in November 1978. Henry Friedman (OCTP) was RADC Project Engineer.

i

TABLE OF CONTENTS

LIST OF ILLUSTRATIONS

iii

EVALUATION

A majority of TWT designs are developed through an iteration of design and test techniques. This results in a significant time delay from concept to the practice and larger development costs due to the "cut and try" techniques used. In an effort to alleviate this problem, relatively sophisticated (and Company Proprietary) computer codes were generated to reduce turn around time and design costs. Since most of these codes were based on Lagrangian and Eulerian formulations, simulations were quite lengthy and costly. This report describes a more cost effective technique which gives good agreement with experimental TWT data. Significant computation time savings have resulted from the use of the polarization model described herein, allowing the designer to practically interact with the resultant simulation. Further, by the availability of this code to Government agencies, it is hoped that this code will enable more quantitative evaluation of future TWT designs.

JOSEPH POLNIASZEK
Project Engineer

1.0 INTRODUCTION

This report presents the basis of a large-signal theory for traveling wave tubes assuming a non-relativistic one-dimensional beam. The theory is expressed in terms of polarization variables which have not been used in large-signal analyses of TWT's before, but can be shown to introduce simplifications in describing certain non-linear effects in the beam dynamics [1,2].

The basic idea of the present formulation can perhaps best be explained by comparison with Lagrangian and Eulerian type formulations which are well known in large-signal TWT calculations. These latter formulations are characterized by non-linear beam dynamics but linear coupling between the beam and the circuit field.

On the other hand the polarization description is characterized by the unique feature that the dynamic equations are linear even in the large-signal domain, whereas the coupling to the circuit field is non-linear. Hence, in the polarization model the non-linear problems are absent in the beam dynamics, but they reappear in the coupling to the circuit field, and to a lesser extent, in the space charge field.

The basic dynamic rf variables are the displacement, or polarization, and the velocity at the displaced position. It can be shown that the harmonics of these variables, for a specified modulation in the beam, decay faster than the harmonics of the rf current and rf space charge used in the common large signal descriptions [3]. This feature, which is unique for the polarization model, has the important practical implication that a smaller number of beam harmonics is sufficient to describe the large signal beam dynamics. In the present work the highest harmonic number included is four, although the basic formulation is for an infinite number of harmonics.

1

2.0 LARGE SIGNAL THEORY WITH POLARIZATION VARIABLES

In this chapter the basic forms of the circuit equations and electronic
equations, expressed in polarization variables, are presented. Let us
first consider the circuit equations.

2.1 CIRCUIT EQUATIONS

The equivalent circuit used in the analysis is shown in Figure 2-1.
The inductance L, capacitance C, and resistance R, all measured per unit
length, are specified as a function of frequency, so that each harmonic
frequency component has its own equivalent circuit. The circuit param-
eters are related to the actual circuit parameters by the relations:

$$L(\omega)C(\omega) = \frac{1}{v_C(\omega)^2} \tag{2-1}$$

$$\frac{L(\omega)}{C(\omega)} = Z_C(\omega)^2 , \tag{2-2}$$

where $v_C(\omega)$ is the phase velocity and $Z_C(\omega)$ the impedance of the circuit,
both referred to a particular frequency ω. Note that the impedance
$Z_C(\omega)$ is specified as the impedance at the circuit radius and not at the
location of the beam.

With these definitions the circuit equations take the form:

$$\frac{\partial I}{\partial z} + \frac{1}{v_C Z_C} \frac{\partial V}{\partial t} = \frac{\partial I_{in}}{\partial z} \tag{2-3}$$

$$\frac{\partial V}{\partial z} + \frac{Z_C}{v_C} \frac{\partial I}{\partial t} + RI = 0 , \tag{2-4}$$
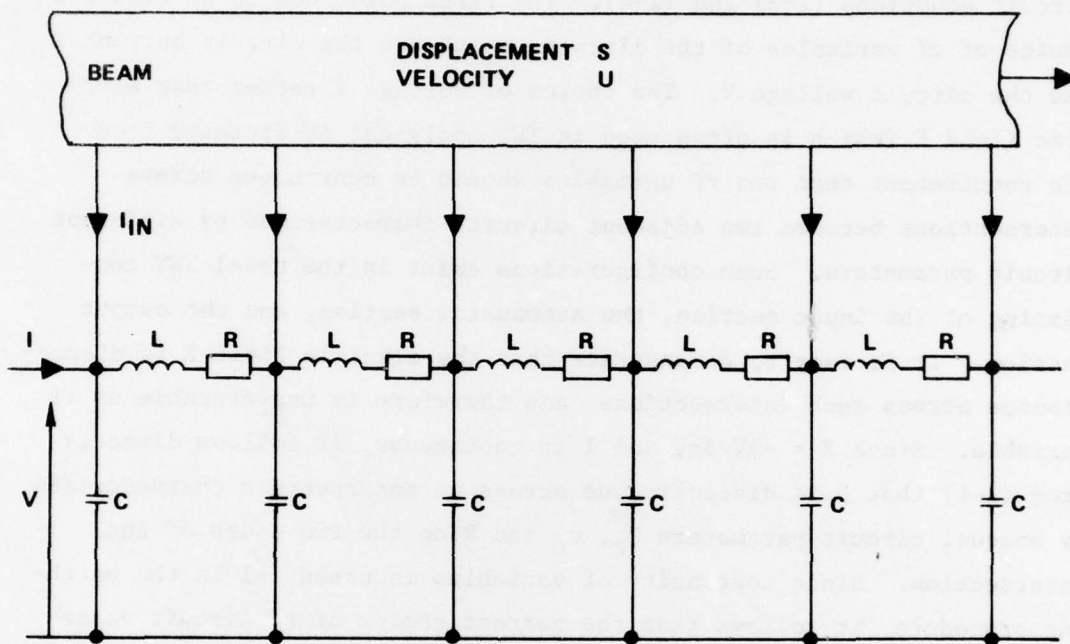
2

Figure 2-1 Equivalent circuit diagram of the circuit interacting with the beam.

where I and V are the circuit current and circuit voltage, respectively. The induced current into the circuit from the beam is I_{in}.

Two important points should be emphasized in connection with the circuit equations (2-3) and (2-4). The first point has to do with the choice of rf variables of the circuit, which are the circuit current I and the circuit voltage V. The choice of voltage V rather than electric field E (which is often used in TWT analyses) is dictated from the requirement that the rf variables should be continuous across intersections between two adjacent circuits characterized by different circuit parameters. Such configurations exist in the usual TWT consisting of the input section, the attenuator section, and the output section. It is easy to demonstrate that the electric field E is discontinuous across such intersections, and therefore is unacceptable as rf variable. Since $E = -\partial V/\partial z$, and I is continuous, it follows directly from (2-4) that E is discontinuous across an intersection characterized by unequal circuit parameters Z_C, v_C and R on the two sides of the intersection. Since continuity of variables is essential in the matching procedure, it follows that the correct choice of rf circuit variables is I and V, rather than I and E.

The second point to be noticed in connection with (2-3) is that the induced current I_{in} in the circuit from the beam is evaluated somewhat differently from the usual way.

2.1.1 The Driving Current in the Circuit Equation

In the usual theory of TWT's the driving current is taken to be the beam current itself, whereas the circuit impedance is reduced by an appropriate factor, thereby essentially placing the circuit at the position of the electron beam. In the present theory a different and more consistent procedure is followed, in which the finite spacing

4

between circuit and beam is accounted for by a coupling coefficient, much in the same way as usually done in klystrons.

The induced current flowing in the circuit is obtained from the integral:

$$I(z_o, t)_{in} = - \int_x f(x - z_o) \, I_b(x, t) dx \qquad (2-5)$$

In this equation, $I_b(x, t)$ is the beam current density, $f(x - z_o)$ is a characteristic response function of the circuit defined in the following way. With reference to Figure 2-2 we visualize a hypothetical gap cut in the circuit at the position z_o, and a voltage of one volt applied across the gap. The function $f(x - z_o)$ is then the longitudinal component of the electric field at the beam position, arising from this voltage. In the one-dimensional theory an averaged value of $f(x - z_o)$ across the beam is used.

According to (2-5) the induced current at z_o is not equal to the beam current at z_o (possibly modified by a constant factor), but rather obtained by adding weighed contributions from the beam current around the position z_o. Therefore, the induced current is a smoothed, or filtered version of the beam current.

The Ramo Equation (2-5) has to be reformulated to fit the polarization model. The following equation applies:

$$\frac{\partial I(z_o, t_o)}{\partial z_o} = \frac{I_o}{v_o} \int_{x_o} f'[x_o + s(x_o, t_o) - z_o] \frac{\partial s(x_o, t_o)}{\partial t_o} \, dx_o, \qquad (2-6)$$

5

HYPOTHETICAL CUT WITH ΔV = 1 VOLT

I_b (x, t)

a

b

$f(x-z_o)$

$x-z_o$

z_o x
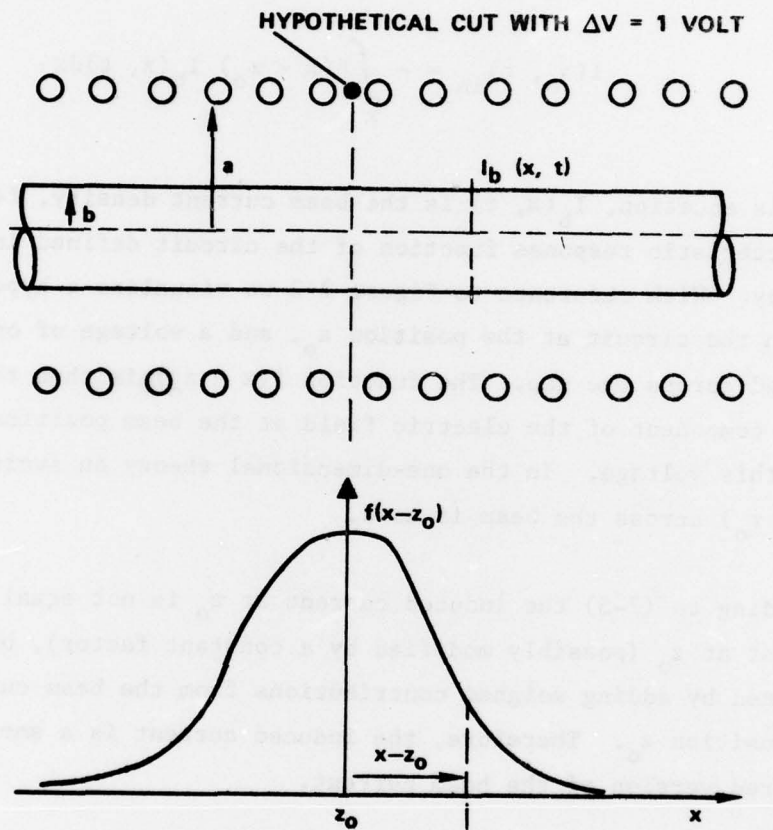
Figure 2-2   Schematic representation of the TWT circuit
and beam, and the definition of coupling
function $f(x - z_o)$.

where x_o is the undisplaced coordinate and $s(x_o, t_o)$ is the displacement, defined by

$$s(x_o, t_o) = x - x_o \qquad (2\text{-}7)$$

Equation (2-6) is valid with overtaking included. The set of independent variables x_o and t_o represent the undisplaced coordinates, i.e., the reference position and time for an unmodulated electron. Note that in (2-6) the response function has to be taken at the displaced position $x_o + s(x_o, t_o)$. Hence, the equation is non-linear, representing exactly the non-linear beam-to-circuit coupling discussed earlier.

The integration over x_o takes place over a sufficiently large interval around z_o to include all non-zero values of the response function.

2.2 ELECTRONIC EQUATIONS

In the polarization model the large signal electronic equations have the form

$$\frac{\partial u(z_o, t_o)}{\partial t_o} + v_o \frac{\partial u(z_o, t_o)}{\partial z_o} = -\eta E[z_o + s(z_o, t_o), t_o] \qquad (2\text{-}8)$$

$$\frac{\partial s(z_o, t_o)}{\partial t_o} + v_o \frac{\partial s(z_o, t_o)}{\partial z_o} - u(z_o, t_o) = 0 \qquad (2\text{-}9)$$

The electric field E in the driving term in (2-8) is taken at the displaced beam position rendering this term non-linear. The field consists of the circuit field E_C at the beam position and the space charge field E_s.

$$E[z_o + s(z_o,t_o),t_o] = E_C[z_o + s(z_o,t_o),t_o] + E_S[z_o + s(z_o,t_o),t_o]$$

$$(2-10)$$

These are given by the following expressions, respectively:

$$E_C[z_o + s(z_o,t_o),t_o] = -\int_{x_o} f'[z_o + s(z_o,t_o) - x_o] \, V(x_o,t_o) dx_o$$

$$(2-11)$$

$$\eta E_S[z_o + s(z_o,t_o),t_o] = -j\omega_p^2 \frac{1}{2\pi} \int_{k=-\infty}^{\infty} \frac{R(k)^2}{k} e^{-jk[z_o + s(z_o,t_o)]} \cdot$$

$$\int_{x_o=-\infty}^{\infty} e^{jk[x_o + s(x_o,t_o)]} dx_o \, dk$$

$$(2-12)$$

In (2-11), the function $f[z_o + s(z_o,t_o) - x_o]$ is the same response function as in (2-6), expressing the simple fact that reciprocity applies with regard to coupling between beam and circuit.

In (2-12) the left side is the longitudinal space charge field averaged over the beam cross section, with the plasma reduction factor $R(k)^2$ specified by:

$$R(k)^2 = R(kb, ka)^2 = 1 - \frac{2I_1(kb) \, G_{10}(kb, ka)}{I_0(ka)}$$

$$(2-13)$$

8

where

$$G_{10}(kb, \ ka) = I_1(kb) \ K_o(ka) + K_1(kb) \ I_o(ka) \qquad (2\text{-}14)$$

This is the plasma reduction factor for a beam constrained to motion in the longitudinal direction only (confined flow) assuming constant current density across the beam.

In the subsequent analysis it is convenient to operate with the Fourier transform $f(k)$ of the response function $f(z_o)$. By definition

$$f(z_o) = \frac{1}{2\pi} \int\limits_{k=-\infty}^{\infty} f(k) e^{-jkz_o} \ dk \qquad (2\text{-}15)$$

so that

$$f'(x_o + s(x_o, \ t_o) - z_o) = -\frac{j}{2\pi} \int\limits_{k=-\infty}^{\infty} kf(k) e^{-jk[x_o + s(x_o, t_o) - z_o]} \ dk$$

$$(2\text{-}16)$$

The Fourier transform $f(k)$ appearing in these equations is obtained by solving the appropriate field problem for the configuration shown in Figure 1-2. The response function averaged over the beam cross section has the Fourier transform:

$$f(k) = f(kb, \ ka) = \frac{2I_1(kb)}{kb} \ \frac{1}{I_o(ka)} \qquad (2\text{-}17)$$

The preceding discussion shows that the overall set of circuit and beam equations are expressed in terms of two characteristic functions of the

9

wave number k, namely the plasma reduction factor R(k) defined in (2-13), and the coupling coefficient f(k) defined by (2-17). In contrast to usual TWT analyses the present theory accounts for the fact that the wave number k is complex, which implies that R(k) as well as f(k) are also complex. Hence, there are small but noticeable differences between the basic models used in the present theory and usual TWT theory. These differences show up even in the small signal results, with small modifications in the gain as well as synchronization conditions.

2.3 INTRODUCTION OF NORMALIZED VARIABLES AND EXPANSION IN HARMONICS

The following normalized variables are used in the theory. Independent normalized variables:

$$Z_o = \beta_e \, z_o \qquad\qquad (2\text{-}18)$$

$$T_o = \omega t_o \qquad\qquad (2\text{-}19)$$

$$K = \frac{k}{\beta_e} , \qquad\qquad (2\text{-}20)$$

where ω is the fundamental frequency and where

$$\beta_e = \frac{\omega}{v_o} \qquad\qquad (2\text{-}21)$$

The normalized rf variables of the circuit are:

$$v(z_o, \, T_o) = \frac{V(z_o, \, t_o)}{V_o} \qquad\qquad (2\text{-}22)$$

10

$$i(Z_o, T_o) = \frac{I(z_o, t_o)}{I_o} \tag{2-23}$$

and those of the beam:

$$U(Z_o, T_o) = \frac{u(z_o, t_o)}{v_o} \tag{2-24}$$

$$S(Z_o, T_o) = \beta_e \, s(z_o, t_o) \tag{2-25}$$

In addition to the normalized displacement $S(Z_o, T_o)$ the following variable is introduced:

$$\phi(K, Z_o, T_o) = j \frac{1}{K} \left[e^{-jKS(Z_o, T_o)} - 1 \right] \tag{2-26}$$

The inverse relation is:

$$e^{-jKS(Z_o, T_o)} = 1 - jK\Phi(K, Z_o, T_o) \tag{2-27}$$

Apparently, for small signals:

$$\lim_{S \to o} \phi(K, Z_o, T_o) = S(Z_o, T_o) \tag{2-28}$$

The function $\phi(K, Z_o, T_o)$ is seen to represent the non-linear effects in the circuit equation as well as the electronic equation.

Since the rf variables are periodic in time, they can be expanded in harmonics as follows:

$$v(Z_o, T_o) = \sum_{-\infty}^{\infty} \hat{v}_n(Z_o) e^{jnT_o} \qquad (2\text{-}29)$$

$$i(Z_o, T_o) = \sum_{-\infty}^{\infty} \hat{i}_n(Z_o) e^{jnT_o} \qquad (2\text{-}30)$$

$$U(Z_o, T_o) = \sum_{-\infty}^{\infty} \hat{U}_n(Z_o) e^{jnT_o} \qquad (2\text{-}31)$$

$$S(Z_o, T_o) = \sum_{-\infty}^{\infty} \hat{S}_n(Z_o) e^{jnT_o} \qquad (2\text{-}32)$$

$$\Phi(K, Z_o, T_o) = \sum_{-\infty}^{\infty} \hat{\Phi}_n(K, Z_o) e^{jnT_o} \qquad (2\text{-}33)$$

In these equations $\hat{v}_n(Z_o)$, $\hat{i}_n(Z_o)$, etc are the complex amplitudes of the nth harmonics.

Substitution of these variables into the circuit equations (2-3) and (2-4) and the electronic equations (2-8) and (2-9), followed by separation of these into harmonic components, results in the overall basic large signal equations specified in the next section.

2.4 HARMONIC SET OF LARGE SIGNAL EQUATIONS

Following the procedure outlined in the preceding discussion, we obtain the following set of large signal equations. The circuit equations for the nth harmonic component are given by:

12

Linear

$$\frac{d\hat{v}_n}{dZ_o} + G_o Z_{Cn}\left(\frac{v_o}{v_{Cn}}\right) jn\kappa_n \hat{i}_n = 0 \qquad (2\text{-}34)$$

Linear
Part

$$\frac{d\hat{i}_n}{dZ_o} + \frac{1}{G_o Z_{Cn}}\left(\frac{v_o}{v_{Cn}}\right) jn\hat{v}_n - n\frac{1}{2\pi}\int_{K=-\infty}^{\infty} Kf(K)e^{-jKZ_o}$$

$$\int_{X_o=-\infty}^{\infty} \hat{S}_n(X_o)e^{jKX_o} dX_o dK$$

Non-
linear
coupling
term

$$= j\sum_{q=-\infty}^{\infty} q\, \frac{1}{2\pi}\int_{K=-\infty}^{\infty} K^2 f(K\beta_e)e^{-jKZ_o}$$

$$\int_{X_o=-\infty}^{\infty} \hat{S}_q(X_o)\hat{\phi}_{n-q}(-K, X_o)e^{jKX_o} dX_o dK \qquad (2\text{-}35)$$

The linear part of the coupling term is retained on the left-hand side
of (2-35), whereas the non-linear right-hand coupling turn is identi-
fied by the dotted outline. The parameters G_o and κ_n appearing in the
circuit equations are defined by:

$$G_o = \frac{I_o}{V_o} \qquad (2\text{-}36)$$

$$\kappa_n = 1 - j\,\frac{R_n}{Z_{Cn}\,\beta_{Cn}} \qquad (2\text{-}37)$$

13

$$\beta_{Cn} = \frac{n\omega}{v_{Cn}} \tag{2-38}$$

Hence, κ_n represents the loss parameter of the circuit for the nth harmonic frequency.

Similarly, the electronic equations are specified by:

Linear part

$$\frac{d\hat{U}_n}{dZ_o} + jn\hat{U}_n + \Omega_p^2 \frac{1}{2\pi} \int\limits_{k=-\infty}^{\infty} R(K)^2 e^{-jKZ_o} \int\limits_{X_o=-\infty}^{\infty} \hat{S}_n(X_o) e^{jKX_o} dX_o \, dK$$

$$+ \frac{j}{2} \frac{1}{2\pi} \int\limits_{k=-\infty}^{\infty} Kf(K) e^{-jKZ_o} \int\limits_{X_o=-\infty}^{\infty} \hat{v}_n(X_o) e^{jKX_o} dX_o \, dK \tag{2-39}$$

Non-linear coupling term

$$= \frac{j}{2} \frac{1}{\pi} \int\limits_{K=-\infty}^{\infty} Kf(K) e^{-jKZ_o} \int\limits_{X_o=-\infty}^{\infty} \sum_{q=-\infty}^{\infty} \hat{\phi}_{n-q}(K, Z_o) \hat{v}_q(X_o) e^{jKX_o} dX_o \, dK$$

$$- \Omega_p^2 \frac{1}{\pi} \int\limits_{K=-\infty}^{\infty} R(K)^2 e^{-jKZ_o} \int\limits_{X_o=-\infty}^{\infty} \sum_{q=-\infty}^{\infty} \left[\hat{\phi}_{n-q}(K, Z_o) - \hat{\phi}_{n-q}(-K, X_o) \right] \frac{d\hat{S}_q(X_o)}{dX_o} e^{jKX_o} dX_o \, dK$$

Non-linear space charge field

$$- j\Omega_p^2 \frac{1}{\pi} \int\limits_{K=-\infty}^{\infty} KR(K)^2 e^{-jKZ_o} \int\limits_{X_o=-\infty}^{\infty} \sum_{q=-\infty}^{\infty} \sum_{p=-\infty}^{\infty} \hat{\phi}_{n-p}(K, Z_o) \hat{\phi}(-K, X_o) \frac{d\hat{S}_q(X_o)}{dX_o} e^{jKX_o} dX_o \, dK$$

$$\frac{d\hat{S}_n}{dZ_o} + jn\hat{S}_n - \hat{U}_n = 0 \tag{2-40}$$

14

Again, the non-linear part of (2-39) is identified by the dotted out-
line. The first non-linear term arises from the non-linearities in the
beam to circuit coupling. The second and third terms are associated
with non-linearities in the space charge field.

In these equations the parameter Ω_p is the __normalized__ plasma frequency
of the beam

$$\Omega_p = \frac{\omega_p}{\omega} \tag{2-41}$$

The non-linear parts of the circuit equation (2-35) and the electronic
equation (2-39) are expressed as superpositions of cross-coupling
terms between the various harmonics of the rf variables $\hat{v}_q(z_o)$, $\hat{S}_q(z_o)$,
and $\hat{\phi}_q(K, z_o)$. The dominant cross-coupling terms are those centered
around the fundamental components $q = +1$ and $q = -1$. As q deviates more
and more from these values, the cross-coupling terms become smaller and
smaller and are finally negligible. Expressed differently, it suffices
to include only a certain number of harmonics. The exact number can
be determined either from the computational procedure, or by making a
reasonable choice based on previous experience from corresponding
klystron programs [1,2]. In the present work we shall take q_{max} (or
n_{max}) equal to four. The fact that the circuit impedance Z_{Cn} is
vanishingly small when the harmonic number n exceeds say two or three,
depending on the helix design, implies that the corresponding circuit
rf variables $\hat{v}_n(z_o)$ and $\hat{i}_n(z_o)$ are negligible. On the other hand the
corresponding dynamic variables $\hat{U}_n(z_o)$, $\hat{S}_n(z_o)$, and $\hat{\phi}_n(K, z_o)$ are not
necessarily negligible, a fact which is easily observed from (2-39) and
(2-40). The higher harmonics in the beam are excited predominantly by
the fundamental circuit field, and to a lesser extent, by the non-
linear space charge field.

It is noted that the basic large signal equations are differential-
integro equations, for the small signal as well as the large signal

15

equations. This formulation is not a consequence of the polarization model as such, but is rather due to the adopted model of beam-to-circuit coupling mechanisms discussed in Chapter 2.1. The differential-integro form gives rise to additional beam loading terms and circuit loading terms that do not appear in conventional TWT theory. Mathematically, the difference manifests itself in the appearance of the plasma reduction factor $R(K)^2$ and the coupling coefficient $f(K)$, which in the present formulation are complex rather than real. It should be pointed out, however, that the imaginary parts of these parameters are quite small compared to the real parts, so that the corresponding corrections are quite small. However, they are noticeable, particularly as far as optimum synchronization conditions are concerned.

The set of large signal Equations (2-34) - (2-40) are equally valid for small signals, which is obtained as a special case by putting the non-linear terms contained within the dotted outlines equal to zero. The major steps in the small signal case will first be treated separately, as it forms a necessary part of the subsequent large signal study.

2.5 SMALL SIGNAL EQUATIONS

According to the foregoing discussion the small signal differential-integro equations are specified as follows:

$$\frac{d\hat{v}_n}{dz_o} + G_o Z_{Cn} \left(\frac{v_o}{v_{Cn}}\right) jn\kappa_n \hat{i}_n = 0 \qquad (2-42)$$

16

$$\frac{d\hat{i}_n}{dZ_o} + \frac{1}{G_o Z_{Cn}} \left(\frac{v_o}{v_{Cn}}\right) jn\hat{v}_n$$

$$- n \frac{1}{2\pi} \int_{K=-\infty}^{\infty} Kf(K)e^{-jKZ_o} \int_{X_o=-\infty}^{\infty} \hat{S}_n(X_o)e^{jKX_o} dX_o \, dK = 0$$

<div style="text-align:right">(2-43)</div>

$$\frac{d\hat{U}_n}{dZ_o} + jn\hat{U}_n + \Omega_p^2 \frac{1}{2\pi} \int_{K=-\infty}^{\infty} R(K)^2 e^{-jKZ_o} \int_{X_o=-\infty}^{\infty} \hat{S}_n(X_o)e^{jKX_o} dX_o \, dK$$

$$+ \frac{1}{2} \frac{1}{2\pi} \int_{K=-\infty}^{\infty} Kf(K)e^{-jKZ_o} \int_{X_o=-\infty}^{\infty} \hat{v}_n(X_o)e^{jKX_o} dX_o \, dK = 0$$

<div style="text-align:right">(2-44)</div>

$$\frac{d\hat{S}_n}{dZ_o} + jn \, \hat{S}_n - \hat{U}_n = 0$$

<div style="text-align:right">(2-45)</div>

As noted earlier the appearance of double integrals in the small signal equations is a consequence of the adapted TWT model. However, due to the linearity of the equations they can be solved using standard procedures.

2.5.1 Small Signal Solutions for $n \neq 0$.

The small signal solution consists of a superposition of four constituent solutions. Let these be numbered by the superscript i, where

<div style="text-align:center">17</div>

$i = 1, 2, 3, 4$. A particular rf variable, say $\hat{S}_n(z_o)$ is then given by the following expression:

$$\hat{S}_n(Z_o) = \sum_{i=1}^{A} \hat{S}_n^{(i)} e^{-jB_n^{(i)}Z_o}, \qquad n \neq 0 \qquad (2-46)$$

where $B_n^{(i)}$ is the normalized propagation factor of the ith solution. It is related to the actual propagation factor $\beta_n^{(i)}$ by:

$$B_n^{(i)} = \frac{\beta_n^{(i)}}{\beta_e} \qquad (2-47)$$

The amplitude $S_n^{(i)}$ is independent of Z_o. If we consider one of the independent four modes specified by its i-value and evaluate the corresponding double integrals in (2-43) and (2-44) we obtain:

$$\frac{1}{2\pi} \int_{K=-\infty}^{\infty} Kf(K) e^{-jKZ_o} \int_{X_o=-\infty}^{\infty} \hat{S}_n(X_o)^{(i)} e^{jKX_o} dX_o \, dK =$$

$$B_n^{(i)} f\left(B_n^{(i)}\right) \hat{S}_n(Z_o)^{(i)}$$

$$(2-48)$$

$$\frac{1}{2\pi} \int_{K=-\infty}^{\infty} R(K)^2 e^{-jKZ_o} \int_{X_o=-\infty}^{\infty} \hat{S}_n(X_o)^{(i)} e^{jKX_o} dX_o \, dK =$$

$$R\left(B_n^{(i)}\right)^2 \hat{S}_n(Z_o)^{(i)}$$

$$(2-49)$$

18

$$\frac{1}{2\pi} \int_{K=-\infty}^{\infty} Kf(K)e^{-jKZ_o} \int_{X_o=-\infty}^{\infty} \hat{v}_n(X_o)^{(i)} e^{jKX_o} dX_o dK =$$

$$B_n^{(i)} f\left(B_n^{(i)}\right) \hat{v}_n(Z_o)^{(i)}$$

$$(2-50)$$

By this procedure we find that the ith mode of the small-signal set (2-42) - (2-45) is specified by the matrix differential equation:

$$\frac{d}{dZ_o} \hat{\underset{\sim}{a}}_n(Z_o)^{(i)} + \underset{\sim}{M}_n^{(i)} \hat{\underset{\sim}{a}}_n(Z_o)^{(i)} = 0 , \qquad \begin{array}{c} n \neq o \\ i = 1,2,3,4 \end{array} \qquad (2-51)$$

where the column vector $\hat{\underset{\sim}{a}}_n(Z_o)^{(i)}$ represents the rf variables.

$$\hat{\underset{\sim}{a}}_n(Z_o)^{(i)} = \begin{bmatrix} \hat{v}_n(Z_o) \\ \\ \hat{i}_n(Z_o) \\ \hline \\ \hat{U}_n(Z_o) \\ \\ \hat{S}_n(Z_o) \end{bmatrix}^{(i)} \qquad (2-52)$$

The 4 x 4 system matrix $\underset{\sim}{M}_n^{(i)}$ is given by

$$\underset{\sim}{M}_n^{(i)} = \begin{bmatrix} 0 & , & G_o Z_{Cn}\left(\dfrac{v_o}{v_{Cn}}\right) jn\kappa_n & \Bigg| & 0 & , & 0 \\[3ex] \dfrac{1}{G_o Z_{Cn}}\left(\dfrac{v_o}{v_{Cn}}\right) jn & , & 0 & \Bigg| & 0 & , & -n B_n^{(i)} f\left(B_n^{(i)}\right) \\[2ex] \hline \dfrac{j}{2} B_n^{(i)} f\left(B_n^{(i)}\right) & , & 0 & \Bigg| & jn & , & \Omega_p^2 R \left(B_n^{(i)}\right)^2 \\[3ex] 0 & , & 0 & \Bigg| & -1 & , & jn \end{bmatrix} \quad (2\text{-}53)$$

$$n \neq 0$$
$$i = 1, 2, 3, 4$$

The solution of the small signal equation (2-51) is straight forward and given by:

$$\hat{\underset{\sim}{a}}_n(Z_o)^{(i)} = e^{-jB_n^{(i)} Z_o} \underset{\sim}{q}_n^{(i)} \hat{A}_n^{(i)} , \qquad n \neq 0 \qquad (2\text{-}54)$$
$$i = 1, 2, 3, 4$$

where $\hat{A}_n^{(i)}$ is the normal mode amplitude of the ith mode, and where $q_n^{(i)}$ is the corresponding _state vector_. The overall small signal solution is a superposition of the form solutions (2-54).

$$\hat{\underset{\sim}{a}}_n(Z_o) = \sum_{i=1}^{4} \hat{\underset{\sim}{a}}_n(Z_o)^{(i)} = \underset{\sim}{Q}_n e^{-j\underset{\sim}{D}_n Z_o} \hat{\underset{\sim}{A}}_n \qquad n \neq o \qquad (2\text{-}55)$$

where the _state matrix_ $\underset{\sim}{Q}_n$ consists of the four state vectors.

20

$$\underset{\sim}{Q}_n = \begin{bmatrix} q^{(1)}_{\sim n} & q^{(2)}_{\sim n} & q^{(3)}_{\sim n} & q^{(4)}_{\sim n} \end{bmatrix} \qquad n \neq 0 \qquad (2\text{-}56)$$

Furthermore, $\underset{\sim}{D}_n$ is a diagonal matrix containing the propagation factors.

$$\underset{\sim}{D}_n = \begin{bmatrix} B^{(1)}_n & 0 & 0 & 0 \\ 0 & B^{(2)}_n & 0 & 0 \\ 0 & 0 & B^{(3)}_n & 0 \\ 0 & 0 & 0 & B^{(4)}_n \end{bmatrix} \qquad (2\text{-}57)$$

The vector $\underset{\sim}{\hat{A}}_n$ consists of the four mutually independent mode amplitudes $\hat{A}^{(i)}_n$, which are independent of Z_o.

$$\underset{\sim}{A}_n = \begin{bmatrix} \hat{A}^{(1)}_n \\ \hat{A}^{(2)}_n \\ \hat{A}^{(3)}_n \\ \hat{A}^{(4)}_n \end{bmatrix} \qquad (2\text{-}58)$$

Equation (2-55) is the complete and general small signal solution, expressed as a superposition of four independent normal modes. The

21

elements of $\underset{\sim}{D}_n$ and $\underset{\sim}{Q}_n$ are obtained from the appropriate eigenvalue relation, which follows from (2-51). For the ith mode:

$$\left[\underset{\sim}{M}_n^{(i)} - jB_n^{(i)}\,\underset{\sim}{1}\right]\underset{\sim}{q}_n^{(i)} = 0 \qquad n \neq 0 \qquad (2\text{-}59)$$
$$i = 1,\ 2,\ 3,\ 4$$

The propagation factors $B_n^{(i)}$ are obtained by putting the determinant equal to zero.

$$\left|\underset{\sim}{M}_n^{(i)} - jB_n^{(i)}\,\underset{\sim}{1}\right| = 0, \qquad n \neq 0 \qquad (2\text{-}60)$$
$$i = 1,\ 2,\ 3,\ 4$$

In expanded form the the determinant equation is given by:

$$B_n^{(i)^4} - 2nB_n^{(i)^3} + B_n^{(i)^2}\left[n^2 - \Omega_p^2 R_n\left(B_n^{(i)}\right)^2 - n^2\kappa_n\frac{v_o}{v_{Cn}}\right.$$

$$\left.\left(\frac{v_o}{v_{Cn}} - \frac{1}{2}f\left(B_n^{(i)}\right)^2\ G_o Z_{Cn}\right)\right] + B_n^{(i)}\,2\left(\frac{v_o}{v_{Cn}}\right)^2 n^3\kappa_n$$

$$- n^2\kappa_n\left(\frac{v_o}{v_{Cn}}\right)^2\ \left(n^2 - \Omega_p^2 R\left(B_n^{(i)}\right)^2\right)\ = 0$$

$$n \neq 0$$
$$i = 1,\ 2,\ 3,\ 4$$

$$(2\text{-}61)$$

The four solutions of this equation specify the four propagation factors $B_n^{(i)}$ of the nth harmonic component. The corresponding state vectors are given by:

22

$$
\underset{\sim}{q}_n^{(i)} = \begin{bmatrix} \dfrac{-2j}{B_n^{(i)} f\left(B_n^{(i)}\right)} \left[\left(n - B_n^{(i)}\right)^2 - \Omega_p^2 R \left(B_n^{(i)}\right)^2\right] \\[3em] \dfrac{-2j}{G_o Z_{Cn}\left(\dfrac{v_o}{v_{Cn}}\right) n \kappa_n f\left(B_n^{(i)}\right)} \left[\left(n - B_n^{(i)}\right)^2 - \Omega_p^2 R \left(B_n^{(i)}\right)^2\right] \\[3em] j\left(n - B_n^{(i)}\right) \\[2em] 1 \end{bmatrix}
$$

$$
\begin{aligned}
&n \neq 0 \\
&i = 1, 2, 3, 4
\end{aligned}
$$

$$(2\text{-}62)$$

2.5.2 Small Signal Solutions for $n = 0$

The previous equations are valid when $n \neq 0$. For $n = 0$ the system is degenerate, and this case must therefore be treated separately. Equations (2-42) – (2-45) are valid for $n = 0$ but the double integrals (2-45) – (2-50) take different forms. The overall solution for $n = 0$, corresponding to (2-55) for $n \neq 0$, is given by:

$$
\underset{\sim}{\hat{a}}_o(Z_o) = \underset{\sim}{Q}_o(Z_o) \, \underset{\sim}{\hat{A}}_o \, ,
\tag{2-63}
$$

where the state matrix $\underset{\sim}{Q}_o(Z_o)$ is a function of distance Z_o along the circuit.

23

$$\underset{\sim}{Q}_o(z_o) = \begin{bmatrix} -G_o \dfrac{R_o}{\beta_e} Z_o & , & 1 & \bigg| & 0 & 0 \\[2ex] 1 & , & 0 & \bigg| & 0 & 0 \\[2ex] -\dfrac{1}{2} G_o \dfrac{R_o}{\beta_e} Z_o & , & \dfrac{1}{2} & \bigg| & 1 & 1 \\[2ex] -\dfrac{1}{4} G_o \dfrac{R_o}{\beta_e} Z_o^2 & , & \dfrac{Z_o}{2} & \bigg| & Z_o & 1 \end{bmatrix} \qquad (2\text{-}64)$$

The normal mode vector $\hat{\underset{\sim}{A}}_o$ specifies the four mutually independent time-average or "dc" modes corresponding to $n = 0$

$$\hat{\underset{\sim}{A}}_o = \begin{bmatrix} \hat{A}_o^{(1)} \\[2ex] \hat{A}_o^{(2)} \\[2ex] \hat{A}_o^{(3)} \\[2ex] \hat{A}_o^{(4)} \end{bmatrix}, \qquad (2\text{-}65)$$

where four constants $\hat{A}_o^{(1)}$ to $\hat{A}_o^{(4)}$ represents the independent normal mode amplitudes of the $n = 0$ solution.

In normal small signal operation the $n = 0$ mode as well as the harmonic modes corresponding to $n \neq \pm 1$ are not excited. However, they are excited at large signal levels through non-linear effects. Moreover, they can also be excited at small signals as well as large signals

24

through harmonic injection at the input end of the helix. In the present treatment we shall include harmonic injection for $n = 0$, i.e., a "dc injection scheme". The motivation for this is that we like to maintain generality and not exclude the possibility of improving the TWT performance by "dc injection", which would supplement the usual second harmonic or higher harmonic injection schemes.

For this purpose it is appropriate to point out the physical significance of the four $n = 0$ modes, each of which is specified by the corresponding column in the state matrix $Q_o(Z_o)$ in (2-64).

The first mode, with arbitrary normal mode amplitude $\hat{A}_o^{(1)}$ determined by the excitation conditions, is characterized by the first column in (2-64). Apparently, this mode corresponds to a physical situation in which the circuit carries a small dc current $\hat{i}_o = \hat{A}_o^{(1)}$ (the second element in the column). This current gives rise to a dc circuit voltage proportional to the circuit resistance R_o and to distance Z_o along the circuit. The constant voltage gradient arising from the linear variation of voltage along the circuit serves as a driving term in the dynamic equations, causing a linearly varying dc velocity component expressed by the third element in the column. The linearly varying velocity component finally gives rise to a displacement which is proportional to the square of distance along the circuit, as shown by the fourth element in the column.

In summary, this first dc mode has a clear physical significance, but is hardly of much practical significance. Its effect on the large signal dynamics would come from the constant accelerating (or decelerating) dc field arising from the combination of injected dc circuit current and the circuit dc resistance R_o. Aside from the difficulties in injecting dc current, thermal dissipation, etc, the resistance would have to be fairly high in order for this effect to be noticeable. The high dc resistance would probably be detrimental for the rf operation. Hence,

25

it is unlikely that a dc injection scheme based on the first mode is
of any practical value. Moreover, the excitation of this mode directly
from the beam due to non-linear effects under large signal conditions
is also prohibited, provided special arrangements are not made to
allow a dc current to flow in the circuit. This is usually not the case.
Therefore, in the large-signal calculations we shall disregard this
mode altogether, putting $\hat{A}_o^{(1)} = 0$.

The second dc mode, corresponding to the second column of the state
matrix $\underset{\sim}{Q}_o(z_o)$, has no dc current in the circuit but a constant dc voltage
$\hat{v}_o = \hat{A}_o^{(2)}$. The voltage corresponds to a dc velocity change of $A_o^{(2)}/2$
and a linearly changing displacement $A_o^{(2)} z_o/2$, as seen from the two
last elements in the column. This mode could conceivably be used in a
"dc injection scheme". For instance, it would characterize a physical
situation in which the two circuit sections of a normal TWT are not at
the same dc voltage. The difference in voltage corresponds to the
normal mode amplitude $\hat{A}_o^{(2)}$ of the second dc mode. As shown in
Section 2.7.2 the second dc mode is not excited by non-linear effects
in the beam-to-circuit coupling, but only from "dc injection" directly
on the circuit.

The third and fourth dc modes are characterized by zero circuit voltage
and current, as seen directly from (2-64). The third dc mode specifies
a constant change in relative dc velocity given by $\hat{v}_o = \hat{A}_o^{(3)}$, asso-
ciated with a linearly increasing or decreasing displacement. Phys-
ically, this mode can be visualized as arising from a small change in
dc velocity v_o. It follows from the subsequent large signal theory
that the mode basically describes the process of slowing down of the
electrons under large signal operation.

The fourth dc mode represents a constant displacement with no change in
velocity. The physical significance of this mode is less obvious. It
can conceivably be excited through some kind of time delays arising

from non-linear effects under large-signal operation. Regardless of physical interpretations, the third and fourth dc modes corresponding to **n** = 0 are certainly excited under large-signal conditions, as shown in Section 2.7.2, and must be included as part of the overall mode configuration in the large-signal analysis.

2.6 COMPARISON WITH CONVENTIONAL TWT THEORY

In the conventional TWT model the circuit is essentially visualized as being at the <u>same position</u> as the electron beam, with an appropriate reduction in circuit impedance depending on the frequency. The fact that the reduction depends on frequency rather than wave number gives rise to certain deficiencies and shortcomings in the conventional TWT model. We shall briefly discuss these and point out how these short-comings are eliminated in the present model.

The differences between the two models, at least at small signal level, have nothing to do with the use of polarization variables, but arise from a different description of the coupling between beam and circuit. In the present model the coupling is essentially specified by the coupling factor $f\left(B_n^{(i)}\right)$ which appears in the off-diagonal coupling terms in the overall system matrix $\underset{\sim}{M}^{(i)}$ in (2-53). The essential point is that the argument in the $f\left(B_n^{(i)}\right)$ - function is the actual propagation factor of the ith mode. In conventional theory the argument is taken to be equal to $\beta_C = \omega/v_C$, or for the nth harmonic, β_{Cn}. Hence the coupling factor is taken to be the same for all four modes, and is frequency dependent, rather than wavelength dependent as in the present model. At first glance this difference may seem fairly insignificant, because the four propagation factors do not deviate much from the cold circuit propagation factor β_C. This is true under normal operation where the present model yields only slightly different gain response, although the optimum synchronization condition is significantly different. However, the differences first come to proper light

27

when circuits with heavy loss, i.e., attenuators, are considered. In such cases there exists an essential disagreement between conventional TWT theory and the present theory.

As the circuit loss is increased, the loss parameter κ_n defined in (2-37) becomes larger and larger. From consideration of the wave equations (2-59) - (2-62) it is easy to show that in the limit of very large κ_n, the circuit-to-beam coupling disappears for the two circuit modes. These are specified by the propagation factors

$$\lim_{\kappa \to \infty} B_n^{(i)^2} = n^2 \left(\frac{v_o}{v_{Cn}} \right) \kappa_n \to j\infty \tag{2-66}$$

The coupling factor $f\left(B_n^{(i)}\right)$ becomes negligible due to the large argument (see (2-17)).

$$\lim_{B_n^{(i)} \to \infty} f\left(B_n^{(i)}\right) = 0 \tag{2-67}$$

Hence, it follows from (2-53) that the off-diagonal coupling terms disappear, rendering the system completely decoupled from the beam as far as the heavily damped circuit modes are concerned. This is not predicted by the conventional TWT model in which the coupling factors are taken to be independent of the propagation factors.

The remaining two modes in a lossy circuit section are essentially the two space charge waves in the beam, which have a finite non-zero coupling to the lossy circuit because the propagation factors are finite, and therefore $f\left(B_n^{(i)}\right)$ different from zero.

In conclusion, the present model distinguishes itself by its ability to account properly for arbitrarily large loss in the circuit structure

This is a great convenience in numerical calculations of multi-section TWT's, where the same basic equations can be used regardless of their loss.

In addition to this discussion we shall be a little more specific about the fundamental difference between the conventional Pierce model and the present model. It is convenient to use the dispersion relation (2-61) as a basis, since it is easily converted to the Pierce form by changing the coupling factor $f\left(B^{(i)}\right)$ and the plasma reduction factor $R\left(B^{(i)}\right)$ to the approximations used in the Pierce model. In the Pierce model the small signal TWT performance is <u>completely</u> described by specifying <u>four</u> independent parameters: the gain parameter C, the loss parameter d, the velocity parameter b, and the space change parameter QC. Once these are specified, the gain characteristics are completely determined regardless of other details of circuit and beam parameters.

The four basic Pierce parameters are related to the parameters used in the present theory by the following equations:

$$C = \left[\frac{1}{4} G_o Z_C f \left(\frac{v_o}{v_C} \right)^2 \right]^{1/3}$$

$$d = \frac{1}{C} \frac{\alpha}{\beta_e}$$

$$b = \frac{1}{C} \left[\frac{v_o}{v_C} - 1 \right]$$

(2-68)

$$QC = \frac{1}{4C^2} \frac{\Omega_p^2 R(1)^2}{\left[1 + \Omega_p R(1) \right]^2}$$

29

where we consider only the fundamental frequency. In (2-68) α is the loss factor of the helix (imaginary part of the complex cold circuit propagation factor). It is related to the loss factor κ defined in (2-37) by the equation:

$$\kappa = 1 - 2j \frac{\alpha}{\beta_C} \left[1 + \left(\frac{\alpha}{\beta_C} \right)^2 \right]^{1/2} \tag{2-69}$$

The argument v_o/v_C in the coupling coefficient $f(v_o/v_C)$ indicates that in the Pierce theory the normalized propagation factor $B = \beta/\beta_e$ is put equal to $\beta_C/\beta_e = v_o/v_C$. This means that the propagation factor is put equal to the cold circuit propagation factor β_C, thus ensuring that the gain parameter C in (2-68) is evaluated on the basis of the cold inter-action impedance $Z_C f (v_o/v_C)^2$ at the beam position.

The argument of unity in the plasma reduction factor R(1), appearing in (2-68), indicates that in the Pierce theory R is evaluated by putting $B = \beta/\beta_e = 1$, i.e., $\beta = \beta_e$.

Inversion of the equations specified by (2-68) yields the following relations:

$$G_o Z_C f \left(\frac{v_o}{v_C} \right)^2 = 4C^3$$

$$\kappa = 1 - 2j \frac{Cd}{1 + Cb} \left[1 + \left(\frac{Cd}{1 + Cb} \right)^2 \right]^{1/2} = \chi_1(Cd, Cb)$$

$$\tag{2-70}$$

$$\frac{v_o}{v_C} = 1 + Cb = \chi_2(Cb)$$

$$\Omega_p^2 R(1)^2 = \frac{4QC^3}{\left[1 - 2\sqrt{QC^3} \right]^2} = \chi_3(C, QC)$$

30

Let us now express the dispersion relation (2-61) in terms of the four Pierce parameters by substituting from (2-69) and (2-70) into (2-61), putting **n** = 1 and for simplicity omitting the superscript **i**. The result is

$$B^4 - 2B^3 + B^2 \left[1 - \chi_3(C,QC) \frac{R(B)^2}{R(1)^2} \right.$$

$$\left. - \chi_1(Cd,Cb)\chi_2(Cb) \left(\chi_2(Cb) - 2C^3 \frac{f(B)^2}{f\left(\chi_2(Cb)\right)^2} \right) \right]$$

$$+ 2B \, \chi_2(Cb)^2 \chi_1(Cd,Cb)$$

(2-71)

$$- \chi_2(Cb)^2 \chi_1(Cd,Cb) \left[1 - \chi_3(C,QC) \frac{R(B)^2}{R(1)^2} \right] = 0$$

This is the small signal dispersion relation valid for the present model, but expressed in terms of the four Pierce parameters defined in (2-68). It is noticed, however, that in addition to these parameters, two more parameters are needed, namely:

a) Modified coupling parameter:

$$\zeta_1 = \frac{f(B)^2}{f\left(\chi_2(Cb)\right)^2}$$

(2-72)

b) Modified space **charge** parameter:

$$\zeta_2 = \frac{R(B)^2}{R(1)^2}$$

(2-73)

31

The essential difference between the present model and Pierce's model can be appreciated from this exposition. In the Pierce model the factors ζ_1 and ζ_2 are both approximated by putting them equal to unity. Inspection of the dispersion relation (2-71) in this approximation reveals that the four propagation factors are specified fully by the four Pierce parameters C, d, b, and QC. As an example, this model predicts identical gain response for two TWT designs with different circuit radii (and possibly different beam radii as well) provided the four basic Pierce parameters are the same in both cases. And this may very well be possible, since a larger circuit diameter can be offset by a basically larger interaction impedance measured at the circuit, so that the interaction impedance is the same at the position of the beam, i.e., the gain parameter C is the same.

In the present model the four basic Pierce parameters must be supplemented by the parameters ζ_1 and ζ_2 defined in (2-72) and (2-73). These are, by themselves, functions of B, or more specifically, functions of βb and βa, which can be expressed as $B(\beta_e b)$ and $B(\beta_e a)$, respectively. Hence, as far as dependence on TWT parameters are concerned, ζ_1 and ζ_2 are functions of the normalized beam and circuit radii $\beta_e b$ and $\beta_e a$.

Hence, we reach the conclusion that our TWT model requires six basic parameters rather than the four required in the Pierce model. The additional parameters are the normalized beam and circuit radii $\beta_e b$ and $\beta_e a$. These are not required in Pierce's model.

As an example consider two TWT designs both having the same Pierce parameters C, d, b, and QC, but different normalized beam and circuit radii. The Pierce model gives identical gain characteristics for these two designs, whereas the present model predicts a difference in gain depending on the normalized beam and circuit radii in the two designs.

32

The circumstance that the two factors ζ_1 and ζ_2 for a particular mode depend on the actual propagation factor β as well, leads us to the conclusion that the differences in gain characteristics obtained from the two models will be larger, the more the complex propagation factor β deviates from β_e and β_C. Therefore, in high-gain tubes and in attenuating sections we expect fairly large differences between the two models.

2.7   LARGE SIGNAL SOLUTION

The large signal equations are given by (2-34) - (2-39) which also contained the small signal equations discussed as a special case in the preceding sections. The motivation for solving the small signal case in detail is not **dictated merely from interest in small signal response**, but more from the fact that certain small signal parameters are needed in the subsequent large signal solutions.

In view of the fact that the left hand sides of the general large signal equations are identical with the small signal equations (2-42) - (2-45), we can take the general large signal solution to be essentially of the same form as the small signal solution (2-55) and (2-63), namely:

$$\hat{\underset{\sim}{a}}_{\mathbf{n}}(Z_o) = \underset{\sim}{Q}_{\mathbf{n}} e^{-j \underset{\sim}{D}_{\mathbf{n}} z_o} \hat{\underset{\sim}{A}}_{\mathbf{n}}(Z_o) \qquad \mathbf{n} \neq 0 \qquad (2\text{-}74)$$

$$\underset{\sim}{a}_o(Z_o) = \underset{\sim}{Q}_o(Z_o)\, \hat{\underset{\sim}{A}}_o(Z_o) \qquad \mathbf{n} = 0 \qquad (2\text{-}75)$$

The state matrices $\underset{\sim}{Q}_{\mathbf{n}}$ and $\underset{\sim}{Q}_o(Z_o)$ and the propagation factors $\underset{\sim}{D}_{\mathbf{n}}$ are identical in the small and large signal case. The large-signal expressions (2-74) and (2-75) differ from the small signal expressions only in the fact that the normal mode amplitude vectors $\hat{\underset{\sim}{A}}_{\mathbf{n}}(Z_o)$ and $\hat{\underset{\sim}{A}}_o(Z_o)$ are taken to be functions of distance Z_o. In the small signal case these vectors **are constant. The variations of the normal mode**

33

amplitudes are caused by the non-linear interactions between modes.
These manifest themselves as saturation effects in the fundamental
component (the corresponding vector $\hat{\underset{\sim}{A}}_1(Z_o)$ becomes smaller as the
signal amplitude grows along the circuit), and in non-linear excitation
of higher harmonics and intermodulation components (the corresponding
vectors $\hat{\underset{\sim}{A}}_n(Z_o)$ grow along the tube).

The essence of the large signal calculations is therefore to determine
the variations of the normal mode vectors $\hat{\underset{\sim}{A}}_n(Z_o)$ and $\hat{\underset{\sim}{A}}_o(Z_o)$ along the
length of the tube for the fundamental component and all harmonics of
interest. Once this has been achieved the general large signal solution
for these nth harmonic is given by (2-74), and for the time average
component by (2-75). The overall large signal solution is obtained by
superposing the harmonics:

$$
\begin{aligned}
\hat{\underset{\sim}{a}}(Z_o,T_o) &= \sum_{n=-\infty}^{\infty} \hat{\underset{\sim}{a}}_n(Z_o) e^{jnT_o} = \hat{\underset{\sim}{a}}_o(Z_o) + \sum_{n \neq 0} \hat{\underset{\sim}{a}}_n(Z_o) e^{jnT_o} \\
&= \underset{\sim}{Q}_o(Z_o)\hat{\underset{\sim}{A}}_o(Z_o) + \sum_{n \neq 0} \underset{\sim}{Q}_n e^{-j\underset{\sim}{D}_n Z_o} \hat{\underset{\sim}{A}}_n(Z_o) e^{jnT_o}
\end{aligned}
$$

$$(2-76)$$

It should be emphasized that the assumed form of the large signal
solutions (2-74) and (2-75) are not approximations, but perfectly
valid at all signal levels. The normal mode amplitudes $\hat{\underset{\sim}{A}}_n(Z_o)$ and
$\hat{\underset{\sim}{A}}_o(Z_o)$ contain the necessary large signal information of _amplitude_ as
well as _phase_ variations of all four modes and all harmonics.

34

2.7.1 Differential Equations for the Large Signal Normal Mode Amplitudes

Mathematical processing of the large signal equations (2-34) – (2-39) results in the following differential equations for the normal mode amplitudes defined in (2-74) and (2-75):

$$\frac{d\hat{\underset{\sim}{A}}_{n}(Z_{o})}{dZ_{o}} = e^{jD_{\underset{\sim}{n}}Z_{o}} \, Q_{\underset{\sim}{n}}^{-1} \, \hat{\underset{\sim}{F}}_{n}(Z_{o}) \qquad n \neq 0 \tag{2-77}$$

$$\frac{d\hat{\underset{\sim}{A}}_{o}(Z_{o})}{dZ_{o}} = Q_{\underset{\sim}{o}}(Z_{o})^{-1} \, \hat{\underset{\sim}{F}}_{o}(z_{o}) \qquad n = 0 \tag{2-78}$$

The vectors $\hat{\underset{\sim}{F}}_{n}(z_{o})$ and $\hat{\underset{\sim}{F}}_{o}(z_{o})$ are non-linear driving terms which are zero in the small signal case. In general:

$$\hat{\underset{\sim}{F}}_{n}(Z_{o}) = \begin{bmatrix} 0 \\ H_{2n}(Z_{o}) \\ H_{3n}(Z_{o}) \\ 0 \end{bmatrix} \qquad n \neq 0 \tag{2-79}$$

$$\hat{\underset{\sim}{F}}_{o}(Z_{o}) = \begin{bmatrix} 0 \\ 0 \\ H_{3o}(Z_{o}) \\ 0 \end{bmatrix} \qquad n = 0 \tag{2-80}$$

The elements $H_{2_{nl}}$ H_{3n} and H_{3o} appearing in these vectors will be discussed later.

The differential equations (2-77) and (2-78) can be integrated directly, yielding:

$$\hat{\underset{\sim}{A}}_n(Z_o) = \int_0^{Z_o} e^{jD_{\sim n}x_o} \underset{\sim}{Q}_n^{-1} \hat{\underset{\sim}{F}}_n(x_o) \, dx_o + \hat{\underset{\sim}{A}}_n(o) \qquad (2\text{-}81)$$

$$n \neq 0$$

$$\hat{\underset{\sim}{A}}_o(Z_o) = \int_0^{Z_o} \underset{\sim}{Q}_o(x_o)^{-1} \hat{\underset{\sim}{F}}_o(x_o) \, dx_o + \hat{\underset{\sim}{A}}_o(o) \qquad (2\text{-}82)$$

$$n = 0$$

In these equations $\hat{\underset{\sim}{A}}_n(o)$ and $\hat{\underset{\sim}{A}}_o(o)$ are the initial values of the normal mode vectors at $Z_o = 0$, i.e., of the input end of the circuit. Because of the low signal level at the input, these are identical to the small signal values. Without harmonic injection $\hat{\underset{\sim}{A}}_n(o) = 0$ for $n \neq \pm 1$. With harmonic injection the corresponding vectors $\hat{\underset{\sim}{A}}_n(o)$ are non-zero.

2.7.2 Excitation of the Time Average Modes (n = 0)

The $n = 0$ mode amplitudes are given by (2-82). Evaluation of $\underset{\sim}{Q}_o(z_o)^{-1}$ and use of (2-80) yield the following expressions for the excitations of the "dc modes":

$$\hat{A}_o^{(1)}(Z_o) = \hat{A}_o^{(1)}(o) = \text{constant} \qquad (2\text{-}83)$$

$$\hat{A}_o^{(2)}(Z_o) = \hat{A}_o^{(2)}(o) = \hat{A}_o^{(2)} = \text{constant} \qquad (2\text{-}84)$$

36

$$\hat{A}_o^{(3)}(Z_o) = -\int_0^{Z_o} H_{3o}(x_o) \, dx_o \qquad (2\text{-}85)$$

$$\hat{A}_o^{(4)}(Z_o) = \int_0^{Z_o} x_o H_{3o}(x_o) dx_o \qquad (2\text{-}86)$$

According to these equations the two first modes do not depend on z_o. They are not excited by the non-linearities in the beam, but arise from a possible external application of dc current or dc voltage in the circuit, as was discussed extensively in 2.5.2. On the other hand, the two last dc modes are excited by the non-linear interactions in the beam. As described in 2.5.2 they describe the general **slowing down** process taking place as the signal amplitude (and therefore $H_{3o}(Z_o)$) increases.

As discussed in 2.5.2 the first mode is zero unless the circuit is excited with a dc current, which normally is not practical. Hence, mode 2 is the only one available for a possible "dc injection" scheme, in which an additional dc voltage equal to $\hat{A}_o^{(2)}(o)$ is applied to the circuit.

Using (2-64) and (2-75) in conjunction with (2-83) - (2-86) the actual time-average, or dc, variables are obtained as follows:

In the circuit ("dc injection"):

$$\hat{v}_o(Z_o) = \hat{v}_o(o) = \hat{A}_o^{(2)} = \text{constant} \qquad (2\text{-}87)$$

$$\hat{i}_o(Z_o) = 0 \qquad (2\text{-}88)$$

In the beam:

$$\hat{U}_o(Z_o) = 1/2 \; \hat{A}_o^{(2)} - \int\limits_o^{Z_o} H_{3o}(x_o) \; dx_o \qquad (2\text{-}89)$$

$$\hat{S}_o(Z_o) = \left[\frac{1}{2} \hat{A}_o^{(2)} - \int\limits_o^{Z_o} H_{3o}(x_o) \; dx_o \right] Z_o + \int\limits_o^{Z_o} x_o H_{3o}(x_o) \; dx_o \qquad (2\text{-}90)$$

The relative reduction of **time-average** velocity is specified by $\hat{U}_o(z_o)$ in (2-89), where the first term is due to the extra dc voltage of $\hat{A}_o^{(2)}$ applied on the **circuit** ("dc injection"), **and the second term repre-**sents the slowing down process caused by non-linear effects **during** the signal growth along the beam.

2.7.3 The Non-Linear Driving Terms in the Large Signal Equations.

The non-linear driving terms $\hat{\underset{\sim}{F}}_n(z_o)$ and $\hat{\underset{\sim}{F}}_o(z_o)$ in the large signal equations (2-77) - (2-82) contain the elements $H_{2n}(z_o)$, $H_{3n}(z_o)$, and $H_{3o}(z_o)$, which are obtained from the basic large signal equations (2-35) and (2-39). The summation over q is eliminated by using the following relations:

$$jK \sum_{q=-\infty}^{\infty} q \hat{S}_q(x_o) \hat{\phi}_{n-q}(-K, x_o) = n \left[\hat{\phi}_n(-K, x_o) - \hat{S}_n(x_o) \right] \qquad (2\text{-}91)$$

$$jK \sum_{q=-\infty}^{\infty} \frac{d\hat{S}_q(x_o)}{dx_o} \hat{\phi}_{n-q}(-K, x_o) = \frac{d}{dx_o} \left[\hat{\phi}_n(-K, x_o) - \hat{S}_n(x_o) \right] \qquad (2\text{-}92)$$

Hereby, the expression for $H_{2n}(Z_o)$ simplifies to

$$H_{2n}(z_o) = n \frac{1}{2\pi} \int\limits_{K=-\infty}^{\infty} Kf(K)e^{-jKZ_o}$$

$$(2\text{-}93)$$

$$\int\limits_{x_o=-\infty}^{\infty} \left[\phi_n(-K,x_o) - \hat{S}_n(x_o) \right] e^{jKx_o} dx_o \, dK$$

which is valid for all **n**, including zero. Hence, for **n** = 0

$$H_{2o}(Z_o) = 0 \qquad (2\text{-}94)$$

which we have already made use of in (2-80).

Proceeding to $H_{3n}(z_o)$ we find, after integration by parts:

$$H_{3n}(Z_o) = \frac{j}{2} \sum_{p=-\infty}^{\infty} \frac{1}{2\pi} \int\limits_{K=-\infty}^{\infty} K(K)\hat{\phi}_{n-p}(K,Z_o)e^{-jKZ_o} \int\limits_{x_o=-\infty}^{\infty} \hat{v}_p(x_o)e^{jKx_o} dx_o \, dK$$

$$- \Omega_p^2 \frac{1}{2\pi} \int\limits_{K=-\infty}^{\infty} R(K)^2 e^{-jKZ_o} \int\limits_{x_o=-\infty}^{\infty} \left[\hat{\phi}_n(K,x_o) - \hat{S}_n(x_o) \right] e^{jKx_o} dx_o \, dK$$

$$- j\Omega_p^2 \sum_{p=-\infty}^{\infty} \frac{1}{2\pi} \int\limits_{K=-\infty}^{\infty} KR(K)^2 \hat{\phi}_{n-p}(K,Z_o)e^{-jKZ_o} \int\limits_{x_o=-\infty}^{\infty} \hat{\phi}_p(-K,x_o)e^{jKx_o} dx_o \, dK$$

$$(2\text{-}95)$$

2.7.4 Transformation of the Double Integrals

The non-linear coupling terms H_{2n} and H_{3n} are expressed as double integrals over K and x_o. These are not easily amendable to numerical

computer calculations. Therefore, we have transformed the double integrals to a different form, which is derived as follows:

Let us consider a general double integral of the form:

$$T(z_o) = \frac{1}{2\pi} \int\limits_{K=-\infty}^{\infty} a(K)e^{-jKZ_o}\hat{b}(K,Z_o) \int\limits_{x_o=-\infty}^{\infty} \hat{C}(K,x_o)e^{jKx_o} \, dx_o \, dK$$

(2-96)

All the double integrals in (2-93) and (2-95) are represented by this general expression provided we make the appropriate identifications of the functions $a(K)$, $\hat{b}(K,Z_o)$ and $\hat{C}(K,x_o)$. For instance, the function $a(K)$ represents $Kf(K)$ in (2-93), $Kf(K)$, $R(K)^2$, or $KR(K)^2$ in (2-95). The function $\hat{b}(K,Z_o)$ is unity in (2-93), it is unity or $\hat{\phi}_{n-p}(K,Z_o)$ in (2-95). The function $\hat{C}(K,x_o)$ represents several different variables, such as $\left[\hat{\phi}_n(-K,x_o) - \hat{S}_n(x_o)\right]$, $\hat{v}_p(x_o)$, and $\hat{\phi}_p(-K,x_o)$.

Regardless of which variables are involved, the function $a(K)$ is a slowly varying function of K. The functions $\hat{b}(K,Z_o)$ and $\hat{C}(K,x_o)$ are "wavelike" functions, almost periodic in Z_o and x_o.

Let us make the following expansion of $\hat{C}(K,x_o)$:

$$\hat{C}(K,x_o) = \sum_{\ell} \hat{C}_{\ell}(K_{\ell},x_o)e^{-j\phi_{\ell}(x_o)}$$

(2-97)

where the phase angle $\phi_{\ell}(x_o)$ is chosen so that the preceding factors $\hat{C}_{\ell}(K_{\ell},x_o)$ are slowly varying functions of x_o. With the rf variables represented by the $\hat{C}(K,x_o)$ function, this is always possible. Expanding the slowly varying functions $\hat{C}_{\ell}(K_{\ell},x_o)$ and $\phi_{\ell}(x_o)$ in Taylor series, we can convert the double integral (2-96) to the following form:

40

$$T(z_o) = \sum_{r=0}^{\infty} \frac{1}{r!} \sum_{\ell} \hat{C}_{\ell}(K_{\ell},z_o)^{(r)} j^r e^{-j\phi_{\ell}(z_o)} \frac{d^r}{dK^r} \left[a(K)\hat{b}(K,z_o) \right]_{K_{\ell}}$$

$$K = K_{\ell} = \frac{d\phi_{\ell}}{dz_o}$$

(2-98)

This is an exact transformation of the double integral. However, since we have taken care to expand the "wavelike" function $\hat{C}(K,x_o)$ in the sum (2-97) so that $\hat{C}_{\ell}(K,x_o)$ are __almost__ independent of Z_o, the derivatives of this function are negligible and can be disregarded compared to the first term in the expansion (2-98). This means that the only term to be retained is the r = 0 term. Hence

$$T(Z_o) = \sum_{\ell} \hat{C}_{\ell}(K_{\ell},Z_o) e^{-j\phi_{\ell}(Z_o)} a(K_{\ell})\hat{b}(K_{\ell},Z_o)$$

(2-99)

where

$$K_{\ell} = K_{\ell}(Z_o) = \frac{d\phi_{\ell}}{dZ_o}$$

(2-100)

The approximation (2-99) of the **exact** expression (2-98) corresponds to disregarding the growth or decay of the __amplitude__ of the function $\hat{C}(K,x_o)$ over some typical "interaction length". The interaction length corresponds to the __nominal width__ of the coupling function $f(z_o)$ between circuit and beam (see Figure 2-2), if a(K) represents f(K). In the case that a(K) stands for $R(K)^2$, the interaction length is typically equal to the width of the **Green** function for the space charge field.

Regardless of details, (2-100) is a sufficiently good approximation for evaluation of the non-linear coupling integrals (2-93) and (2-95). The practical problem is then reduced to determination of the functions $\hat{C}_\ell(K_\ell, \dot{x}_o)$ and the phase angles $\phi_\ell(x_o)$ in the expansion (2-97). This information is extracted from the appropriate rf variable representing the $\hat{C}(K, x_o)$ function, as discussed earlier. In most cases the $\hat{\phi}_n(K, x_o)$ functions are involved in this procedure, and a major part of the remaining details is concerned with the expansions of the various harmonics of the $\phi(k, x_o)$ - function defined by (2-26). These expansions are necessary details for the numerical procedure, but do not provide more insight into the architectural structure of the large signal theory and program. They are therefore not included in the present report. Nor are details concerning multi-section TWT's, which are easily handled by the present theory, and considerations of launching conditions and extraction of the rf signal at the output.

REFERENCES

1. T. Wessel-Berg, "Relativistic large signal theory of klystrons using polarization variables", (Unpublished notes prepared for Stanford Linear Acceleration Center, Stanford, California) Computer program developed for use in high power klystron design.

2. T. Wessel-Berg, "Large-signal klystron theory expressed in displacement variables", (Project No. 553, 1217/2A, Swedish Board for Technical Development). Division of Physical Electronics, Norwegian Institute of Technology) Trondheim, Norway.

3. J. E. Rowe, "Non-linear Electron-Wave Interaction Phenomena", Academic Press, New York. 1965.

4. J. R. Pierce, "Traveling-Wave Tubes", D. van Nostrand Company, Inc., 1950.
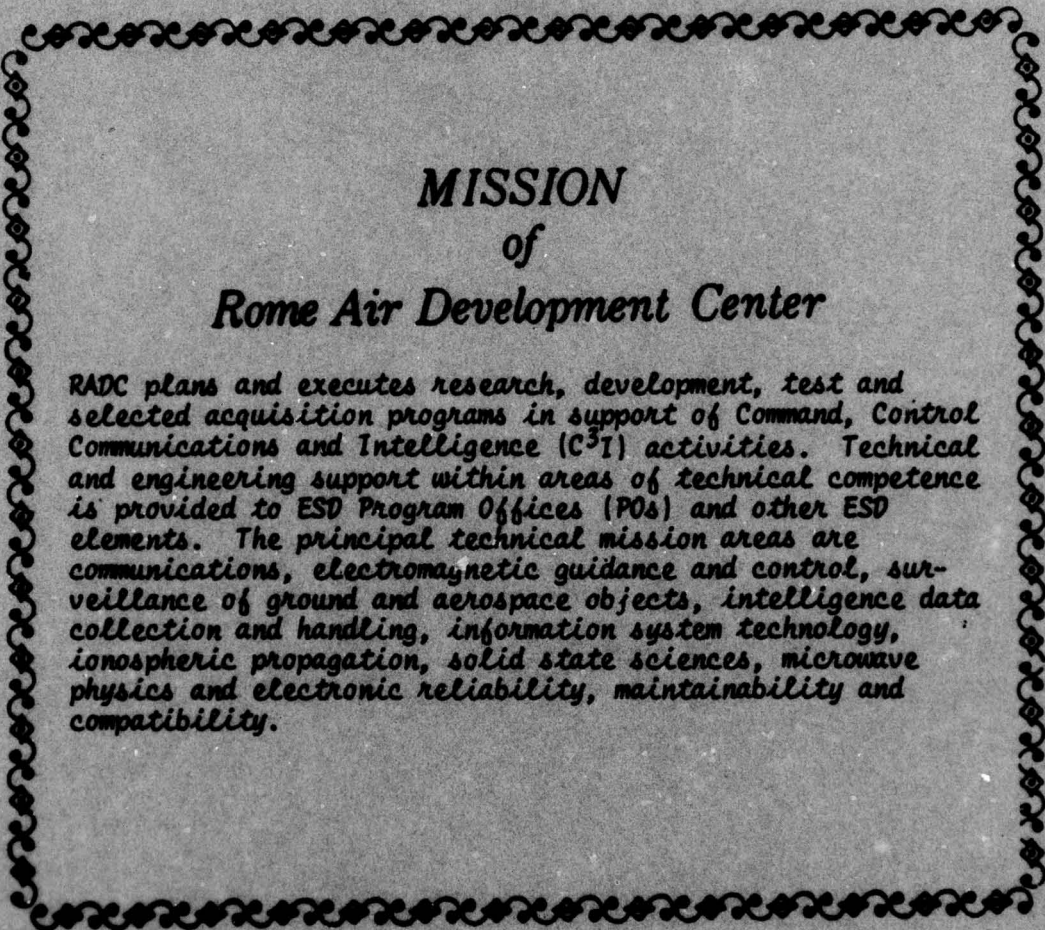
MISSION
of
Rome Air Development Center

RADC plans and executes research, development, test and selected acquisition programs in support of Command, Control Communications and Intelligence (C³I) activities. Technical and engineering support within areas of technical competence is provided to ESD Program Offices (POs) and other ESD elements. The principal technical mission areas are communications, electromagnetic guidance and control, surveillance of ground and aerospace objects, intelligence data collection and handling, information system technology, ionospheric propagation, solid state sciences, microwave physics and electronic reliability, maintainability and compatibility.